Journal of Astronomical Instrumentation, Vol. 5, No. 3 (2016) 1650006 (8 pages)

DOI: 10.1142/S2251171716500069

World Scientific
www.worldscientific.com

ALOHA 1.55 μm Implementation on the CHARA Telescope Array: On-Sky Sensitivity Tests

R. Baudoin*, P. Darré*, J.-T. Gomes*, M. Fabert*, L. Grossard*, L. Delage*, F. Reynaud*,§, N. J. Scott†, J. Sturmann†, T. A. Ten Brummelaar† and V. Coudé du Foresto‡,¶

*Xlim Département Photonique, UMR CNRS 7252, 123 av. Albert Thomas 87060 Limoges, France

†The CHARA Array, Mount Wilson Observatory, Mount Wilson, CA 91023, USA

‡LESIA-CNRS, Observatoire de Paris, 92192 Meudon Cedex, France

§francois.reynaud@xlim.fr

Received 2015 November 18; Revised 2016 February 25; Accepted 2016 February 29; Published 2016 April 29

We intend to implement the ALOHA at 1.55 μm up-conversion interferometer on the CHARA Array. After a full laboratory investigation, a sensitivity evaluation is conducted on several stars using a single interferometric arm in a photometric mode. The on-sky photometric results allows us to calibrate a numerical simulation of the interferometric configuration, and to predict the future performance of ALOHA at 1.55 μm as a function of the seeing conditions.

Keywords: Aperture synthesis, interferometry, non-linear wave mixing, up-conversion, fiber optics.

1. Introduction and General Principle of ALOHA

High resolution imaging instruments are most commonly based on spatial coherence analysis using a telescope array and direct beam combination (Brummelaar *et al.*, 2005; Petrov *et al.*, 2007). One of the current challenges in astronomy is to extend this method to the mid-infrared domain in order to address specific astrophysical topics, for example active galactic nuclei, young stellar objects, formation and evolution of planetary systems. Nowadays, very few instruments, such as MIDI (Leinert *et al.*, 2004), LBTI (Defrère *et al.*, 2015) and MATISSE (Lagarde *et al.*, 2012), are or are planning to address this scientific field using classical techniques to carry out the required beam combination.

We propose an alternative method, called ALOHA (Astronomical Light Optical Hybrid Analysis) (Gomes *et al.*, 2014b), involving non-linear optics to process the light. Figure 1 shows a schematic view of this new kind of instrument. The light collected at the focus plane of each telescope is wavelength shifted by means of a non-linear sum frequency generation (SFG) process (Boyd, 2008) that takes place in a non-linear crystal powered by a laser pump. We define λ_s, λ_p and λ_c as the astronomical light signal, the pump source and the converted signal wavelength, respectively. This way, the converted light reaches a spectral band with shorter wavelengths easier to manage and leads to several advantages. For example, a single set of optical waveguides can be used to transport the optical field with a very high throughput. Using single-mode waveguides also performs spatial filtering with a high rejection efficiency, leading to accurately calibrated fringes (Coudé du Foresto and Ridgway, 1992; Le Bouquin *et al.*, 2011). Furthermore, converting the light to shorter wavelengths drastically reduces the influence of thermal background radiated from all of the elements involved in the whole transmission

¶Current Address: Center for Space and Habitability, Bern University, Switzerland.

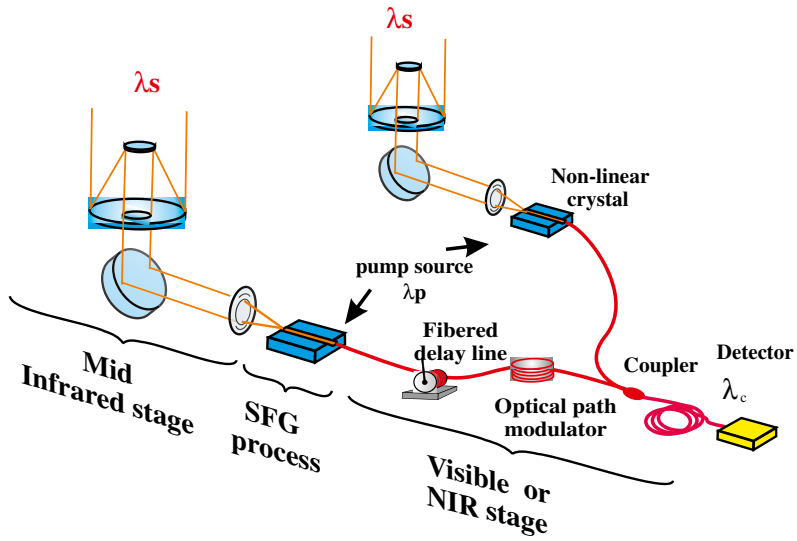

Fig. 1. General principle of ALOHA. The optical fields collected by a set of telescopes are frequency shifted in non-linear crystals into the visible or near infrared bands. The beams are then processed using optical fibers or guided components such as a fibered delay line and an optical path modulator. The two converted beams are mixed in a coupler and the fringe pattern is detected in the time domain by a silicon photon counting detector.

chain, and in particular the mirrors normally used for guiding the beams towards the central facility used in most current instruments. This would result in an increase of the signal-to-noise ratio (SNR) measurement. Last but not least, the up-conversion process allows the use of relatively low-cost and high-performance photon counting detectors with high quantum efficiency, and low dark

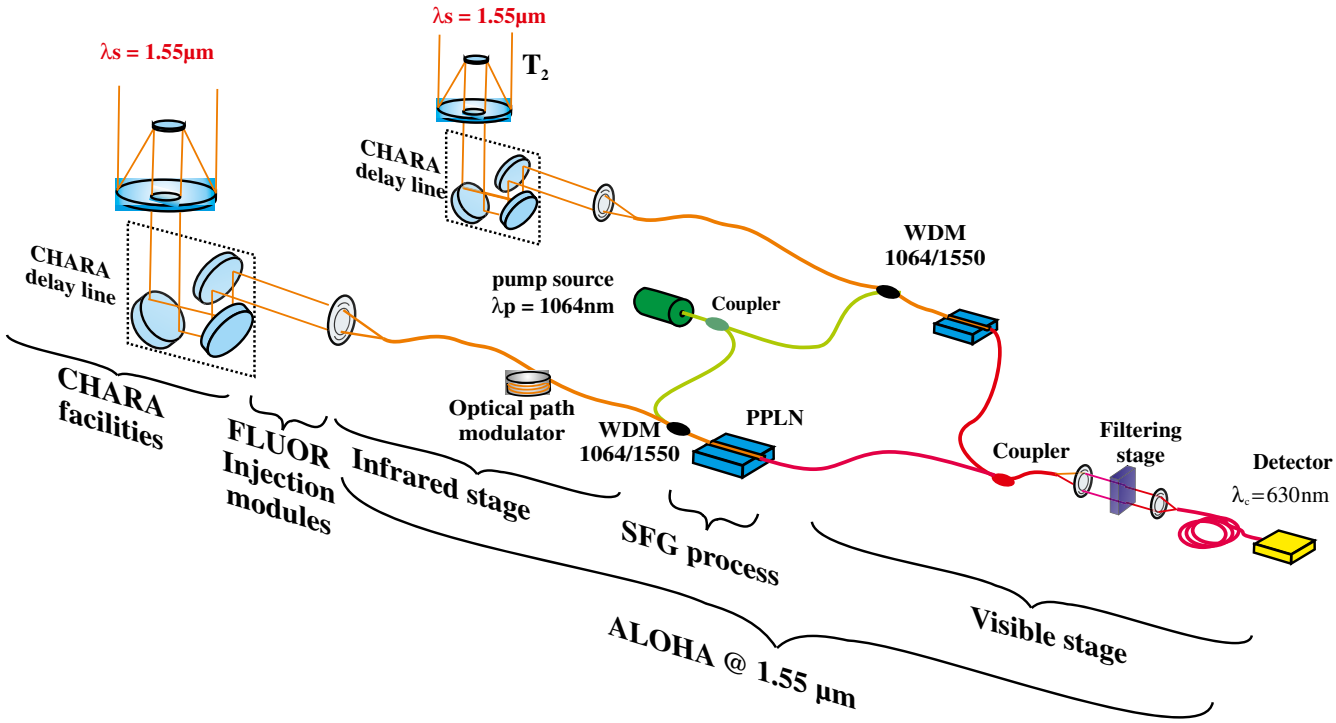

Fig. 2. Interferometric configuration of ALOHA/CHARA to be tested in a near future. The CHARA Array routes the star light beams to the FLUOR injection modules, where they are injected in single-mode polarization maintaining fibers at 1.55 μm. These infrared beams are frequency converted in PPLN crystals into the visible spectral domain. The two converted beams are then mixed in a coupler and spectrally filtered. The fringe pattern is realized in the time domain using an optical path modulator and detected by a photon counting detector.

count, compared to their more expensive equivalents in the infrared.

For more than 10 years, we have performed laboratory experiments on this type of beam combination scheme with the primary intention of checking the validity of this new instrumental concept. With an artificial source, the required fringe contrast and phase closure in low flux configurations have been measured down to the photon counting regime. In order to reduce the experimental complexity, these in-lab preliminary studies used mature technologies developed in the framework of optical communications at 1.55 μm which lies within the astronomical H band. The main results were:

(a) contrast measurements in both high flux and photon counting regimes (Brustlein *et al.*, 2008)
(b) phase closure acquisitions in both high flux (Ceus *et al.*, 2011) and photon counting regimes (Ceus *et al.*, 2013)
(c) laboratory fringes using a black body source (Gomes *et al.*, 2014a).

Our medium-term objective is to get on-sky fringes with the ALOHA instrument at 1.55 μm using two arms of the CHARA Array at Mount Wilson Observatory. The experimental setup of this future experiment is described in Fig. 2.

After propagation through the CHARA Array delay lines, the star beams are injected into single-mode polarization maintaining optical fibers at 1.55 μm using the FLUOR injection modules (Scott *et al.*, 2013). The optical fields at $\lambda_s = 1550$ nm are upconverted in periodically poled lithium niobate (PPLN) crystals fed by a pump laser source at $\lambda_p = 1064$ nm. The converted infrared spectra are limited to the 0.6 nm of the spectral acceptance of the non-linear crystals. The converted optical fields at $\lambda_c = 631$ nm are mixed and spectrally filtered to reject the pump source residues. The fringe pattern is then detected in the temporal domain thanks to an optical path modulator.

In this paper, we report on on-sky sensitivity tests conducted at 1.55 μm on one arm of the CHARA Array coupled to the ALOHA instrument using the FLUOR injection module. These tests are a mandatory step before planning the observation of fringes between two telescopes of the CHARA Array using ALOHA at 1.55 μm.

2. Implementation of One Arm of ALOHA at 1550 nm on the CHARA Array

This work is focused on sensitivity tests to scale a simulation tool to predict the performance of the complete instrument in its interferometric configuration. To this end, only one arm of the future instrument is implemented, as shown in Fig. 3, without the possibility of getting interferometric fringes.

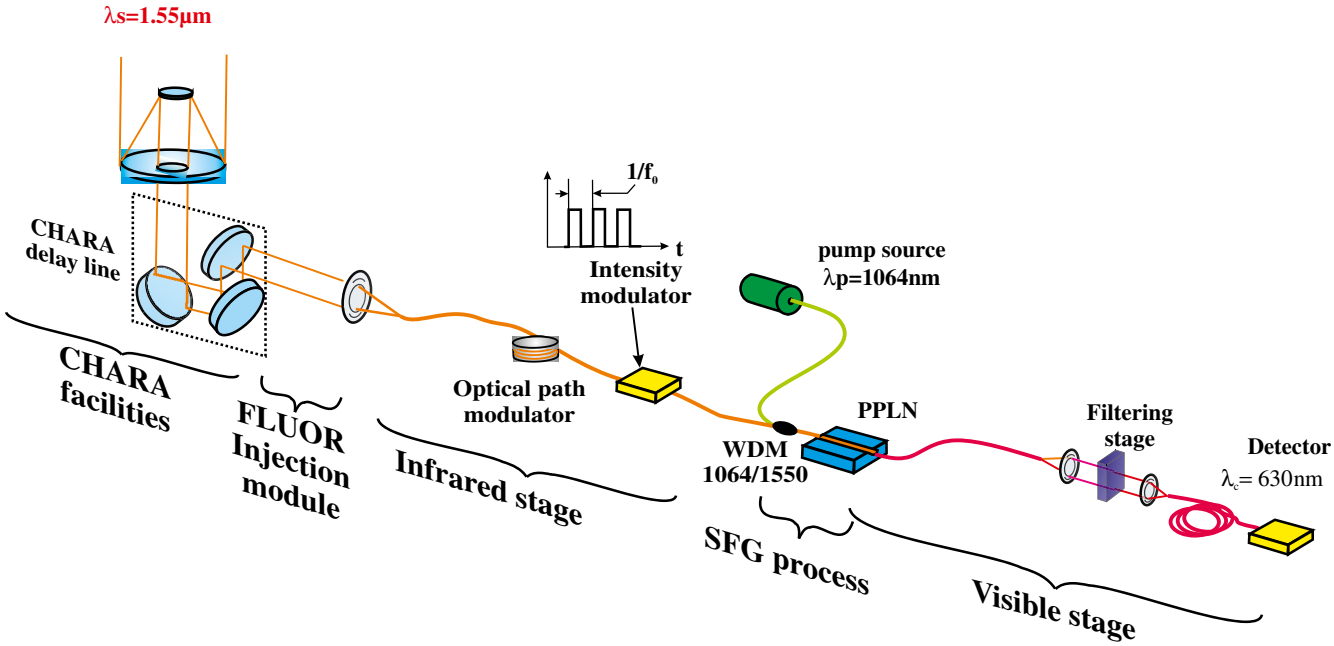

Fig. 3. Photometric configuration of only one arm of ALOHA at 1.55 μm system implemented on the CHARA Array. An intensity modulator in the infrared stage is used to tag the star light signal.

In this configuration, an intensity modulator is added between the fiber optical path modulator and the up-conversion stage. The light flux coming from the star is modulated by a square waveform to increase the SNR of the converted signal detection. This modulator adds well-known losses. Of course, it will not be implemented in the future instrument since the interferometric signal will instead be modulated by the fringe pattern itself.

The input fiber of ALOHA is plugged into the FLUOR injection module. As shown in Fig. 3, a 7 m H-band fiber carries the star light towards the instrument located in the computer room adjacent to the CHARA beam combination laboratory. A raster scan, necessary to optimize the position of the fiber tip at the focus of the injection module, is performed using the fluoride fiber dedicated to the K-band and the FLUOR camera. Then, the K fiber is replaced by the H-band fiber and a final adjustment is then performed manually in order to compensate for differential refraction effects between the two astronomical bands. The intensity modulator is driven by a 50% duty cycle square wave at $f_0 = 200$ Hz. After passing through the frequency conversion stage and the filtering assembly, the beam reaches a silicon avalanche photon counting detector. The electrical output signal is temporally sampled at 200 kHz by a national instrument acquisition system controlled by a LabVIEW VI. The raw data consist of a set of N frames of binary functions $X_i(t)$, each one recorded over an acquisition time τ. These frames are individually processed by a fast Fourier transform to get

$$\widetilde{X_i}(f) = \mathrm{FFT}[X_i(t)]. \tag{1}$$

The synchronization between the intensity modulation and the detection makes possible the coherent integration of $\tilde{X}(f)$ over N frames using

$$\langle \tilde{X}(f) \rangle = \frac{1}{N} \sum_{1}^{N} \tilde{X}_i(f), \tag{2}$$

where $\tilde{X}_i(f)$ is the spectrum of one snapshot measurement and N is the number of frames over which the integration is achieved. We note that $\tilde{X}_i(f)$ cannot be integrated in the full interferometric configuration due to the unpredictable piston error induced by the atmospheric fluctuations. Nevertheless, even in the photometric configuration, the converted astronomical measurement is perturbed by noise resulting from two sources. The first one is the dark count noise, including the intrinsic detector noise and the bias counts optically generated by the up-conversion stage (Pelc *et al.*, 2011). In our case, the dark count noise is in the range of 1000 counts/s. The second one is the photon noise related to the real photons coming from the astronomical source and up-converted in the non-linear stage. For a $H_{\mathrm{mag}} = 0$ stellar source and a seeing close to 1″, approximately 100 photons/s are recorded. Therefore, in our experimental configuration, the standard deviation of the detected counts is mainly due to the dark count noise.

3. Experimental Results

Figure 4 shows two examples of recorded signals obtained on the stars Alpha Boo ($H_{\mathrm{mag}} = -2.8$) and FP Virgo ($H_{\mathrm{mag}} = 1.4$).

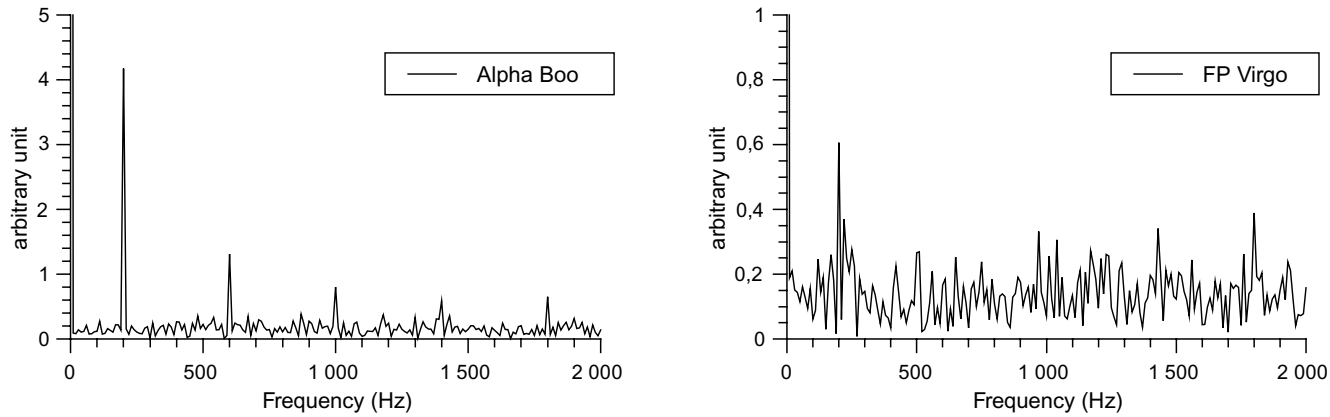

Fig. 4. Plot of the squared modulus of the Fourier Transform of the frames integrated over time ($|\langle \tilde{X}(f) \rangle|^2$), for two stars: Alpha Boo ($H_{\mathrm{mag}} = -2.8$, integration time $\Delta T = 580$ s) and FP Virgo ($H_{\mathrm{mag}} = 1.4$, integration time $\Delta T = 800$ s). The intensity modulator is driven by a square wave at $f_0 = 200$ Hz.

For the bright source Alpha Boo, the intensity modulation peak and its odd harmonics clearly appear at the right frequencies (f_0 and $(2k+1)f_0$). On the contrary, with a fainter object (FP Virgo), this modulation peak signature is weaker, but still visible. To quantify these results, we define the SNR as

$$\mathrm{SNR} = \frac{|\langle \tilde{X}(f_0)\rangle|^2 - \langle N_c\rangle}{\mathrm{RMS}(|\langle \tilde{X}(f)\rangle|^2)} \quad (3)$$

$$\text{where} \quad f \neq (2k+1)f_0 \quad \text{and} \quad k \in \mathbb{N}.$$

This figure of merit measures the ratio between:

- the fundamental peak at f_0 after correction of the shot noise induced by the counting process. Here $\langle N_c\rangle$ is the mean number of counts for each frame and enables us to correct the quantification noise
- the noise evaluated as the fluctuation of the background at the frequencies different to 0, f_0 and its odd harmonics $(2k+1)f_0$ (with $k \in \mathbb{N}$).

Figure 5 shows the evolution of the SNR as a function of the integration time over a $\Delta T = N \cdot \tau$ maximum duration, where $\tau = 100$ ms. In addition, the atmospheric coherence length r_0 is estimated during the integration time by the CHARA seeing monitoring system at 550 nm. The brightest stars are detected easily with a SNR better than 10 in less than 100 s (Fig. 5, left) with an atmospheric coherence length r_0 close to 6 cm. This corresponds to a seeing of approximately 1.9″. For fainter objects (Fig. 5, right), the SNR decreases significantly. To determine the limiting magnitude, we use a SNR = 3 criterion. This way, LN Virgo is the faintest observed source with a seeing of 1.1″ and after an integration time close to $\Delta T = 15$ min. The non-monotonic evolution of the SNR is due to the seeing fluctuations and clouds passing during the measurements. Table 1 summarizes the different photometric test results.

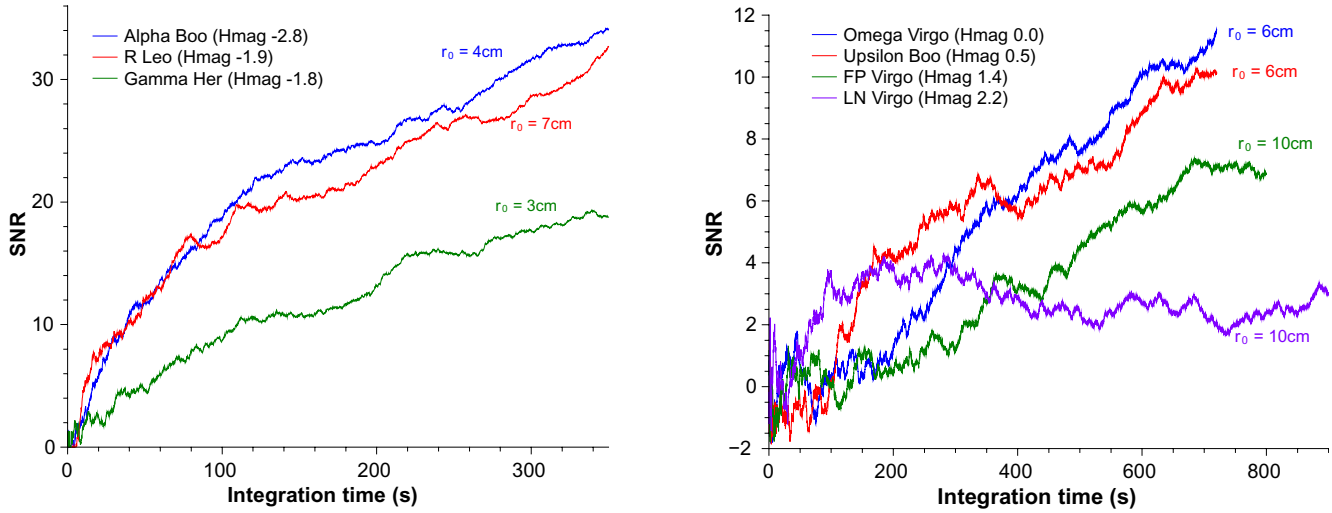

Fig. 5. Evolution of the SNR as a function of the integration time for a set of bright stars (left) and some fainter stars (right). The frame duration is $\tau = 100$ ms. The experimental data were collected during four nights where the seeing conditions will have changed.

Table 1. Summary of the photometric test results.

Stellar source	H_{mag}	Date	Atmospheric coherence length r_0 (cm)[a]	Seeing (arcsec)	Integration time ΔT (s)	SNR
Alpha Boo	−2.8	2014 May 11	4	2.8	350	34.1
R Leo	−1.9	2014 May 12	7	1.6	350	32.7
Gamma Her	−1.8	2014 May 13	3.5	3.2	350	18.8
Omega Virgo	0.0	2014 May 12	6	1.9	720	11.5
Upsilon Boo	0.5	2014 May 12	6	1.9	720	10.1
FP Virgo	1.4	2014 May 14	10	1.1	800	6.4
LN Virgo	2.2	2014 May 14	10	1.1	900	3.0

[a]For each stellar source, the mean value of atmospheric coherence length r_0 is estimated at 550 nm during the integration time.

The global transmission coefficient of the experimental setup strongly depends on the atmospheric turbulence because of the spatial filtering. This global coefficient is given by the product of two terms:

- T_1, the transmission coefficient of the CHARA Array, including its delay lines and the injection of light into the ALOHA single-mode fiber in H band determined from the experimental results presented in Table 1. Note that this transmission coefficient is a function of the atmospheric coherence length r_0.
- T_2, the transmission coefficient from the ALOHA single-mode H band fiber to the detector. This term has been measured in-lab for the experimental configuration presented in Fig. 3, and has been found in the range of 0.1%. This coefficient is obtained considering an unpolarized light at the input of the setup, and the losses added by the intensity modulator.

We developed a numerical model to fit the coefficient T_1 in order to retrieve the SNR evolution obtained experimentally. For this calculation, we took into account:

- the magnitude of the stellar source in H band,
- the transmission coefficient T_2 from the ALOHA single-mode H band fiber to the detector,
- the spectral acceptance and the dark count noise due to the SFG process,
- the experimental conditions such as the integration time, the number of frames N and the atmospheric coherence length r_0,
- the data processing adapted to the photometric configuration.

T_1 is estimated at 5% for a seeing close to 1.1″. Using the numerical model, it is then possible to compute this transmission coefficient for different seeings, the only parameter being the number of spatial modes seen by the primary mirror of the telescope, linked to the atmospheric coherence length r_0. In particular, for an atmospheric coherence length $r_0 = 14\,\text{cm}$ (seeing 0.8″), only one spatial mode is seen, and T_1 should be equal to 10%. This is the highest value reachable with the use of the H fiber of our instrument.

4. Estimation of the Performance of ALOHA/CHARA in the Interferometric Configuration

We have developed a second numerical simulation corresponding to the experimental configuration shown in Fig. 2. The evolution of the SNR in the interferometric configuration is computed as a function of the integration time or as a function of the number of frames N. In this interferometric configuration, the mean number of science photons raises by a factor 6 due to the removal of the intensity modulator and the addition of a second interferometric arm and a coupler in the visible stage.

In this interferometric mode, the piston error induces a random fluctuation of the fringe pattern position. It is therefore necessary to integrate on the squared modulus of the spectrum (incoherent integration) rather than the spectrum itself. The data processing is adapted using the following equations

$$\langle|\tilde{X}(f)|^2\rangle = \frac{1}{N}\sum_{1}^{N}|\tilde{X}_i(f)|^2, \tag{4}$$

$$\text{SNR} = \frac{\langle|\tilde{X}(f_0)|^2\rangle - \langle N_c\rangle}{\text{RMS}(\langle|\tilde{X}(f)|^2\rangle)}, \text{where } f \neq f_0. \tag{5}$$

Table 2 summarizes the differences between the interferometric and photometric configurations.

Using the model of our instrument, it is possible to compute the SNR as a function of the following parameters:

- H_{mag} magnitude of the source
- T_1 evaluated by the photometric tests for a given value of r_0
- the star light converted bandwidth imposed by spectral acceptance of the SFG process
- the global transmission of the ALOHA instrument characterized in laboratory
- the frame duration τ
- the number of frames N over which the integration is performed, inferred from the integration time ΔT and τ.

The piston error due to the atmospheric turbulence is not taken into account in these simulations.

Table 2. Summary of the common parts and differences between the interferometric (Fig. 2) and the photometric (Fig. 3) configurations.

	Interferometric	Photometric
CHARA facilities	same	same
IR stage		+Intensity modulator
SFG stage	same	same
Visible stage	+visible coupler	
Filtering stage	same	same
Detection stage	same	same
Data processing	$\langle\|\tilde{X}(f)\|^2\rangle$	$\|\langle\tilde{X}(f)\rangle\|^2$

Experimentally, it will result in a spreading of the fringe peak in the power spectrum, that can be partly compensated by integration of this fringe peak over several adjacent spectral channels. Moreover, the optical path modulation will be applied over a stroke of some tens of μm during the frame duration τ. According to the narrow spectral acceptance of the SFG process (0.6 nm), this optical path modulation is much smaller than the coherence length of the converted signal. This way, the fringes will be observable with an almost constant contrast all over the scan of each frame when the delay line is set at the zero optical path difference. According to the technical specifications of the CHARA Array, the stability of the instrument would allow integration over more than $\Delta T = 20$ min. Note that the shorter wavelength of the upconverted optical field will not increase the sensitivity to atmospheric turbulence fluctuations or mechanical vibrations as the phase of the infrared signal is merely copied to the visible converted one.

Table 3 shows a comparative analysis of the simulated SNR as a function of the atmospheric coherence length r_0 and the frame duration τ for a $H_{\text{mag}} = 1.5$ source. We have experimentally and numerically determined the minimum SNR threshold equal to 3 for the detection of the observed source in interferometric mode. This way, a $H_{\text{mag}} = 1.5$ source is detectable in all the different cases except for the $r_0 = 6$ cm and $\tau = 100$ ms configuration. Note that the probability to have a seeing better than $2''$ ($r_0 = 6$ cm) in May is greater than 70%, and 34% for a seeing better than $0.8''$ ($r_0 = 14$ cm) (cleardarksky.com, 2016; weather.gc.ca, 2016). These numerical results show that, to optimize the SNR, it is greatly preferable to use longer frame duration.

Table 4 gives the limiting magnitude (defined for SNR = 3) that can be detected in interferometric mode with $\tau = 200$ ms and $N = 6000$, i.e. for an integration time $\Delta T = 20$ min. For very low SNRs, we can expect a decrease in performance due to the atmospheric turbulence. In this case, it would not be possible to integrate the fringe peak spreading over the different spectral channels.

Table 3. Simulated SNR as a function of the seeing and the frame duration τ for a $H_{\text{mag}} = 1.5$ source. Integration time $\Delta T = 20$ min.

Seeing (arcsec)	$r_0 = 6$ cm 1.9	$r_0 = 10$ cm 1.1	$r_0 = 14$ cm 0.8
$\tau = 100$ ms	2.6	25	82
$\tau = 200$ ms	5.0	35	117
$\tau = 400$ ms	6.5	47	163

Table 4. Determination of the limiting magnitude $H_{\text{mag}}^{\text{limit}}$ related to a SNR = 3 as a function of the seeing. These simulations are performed with $\tau = 200$ ms and $N = 6000$, i.e. for an integration time $\Delta T = 20$ min.

Seeing (arcsec)	$r_0 = 3$ cm 3.8	$r_0 = 6$ cm 1.9	$r_0 = 10$ cm 1.1	$r_0 = 14$ cm 0.8
$H_{\text{mag}}^{\text{limit}}$	0.1	1.6	2.8	3.7

5. Discussion and Conclusion

In this paper, we have reported on the implementation of the ALOHA instrument at 1.55 μm on the CHARA Array. ALOHA is an alternative instrument where the astronomical light is frequency shifted from the near infrared to the visible domain thanks to a non-linear process. We conducted the firsts on-sky sensitivity tests on a single arm of the ALOHA/CHARA interferometer, where an intensity modulator has been used to tag the light coming from the astronomical source, before being upconverted in the non-linear stage and detected in the photon counting regime.

We measured the evolution of the SNR as a function of the integration time for several stars from magnitudes ranging from −2.8 to 2.2 in the H band. The converted infrared spectrum is given by the 0.6 nm width of the spectral acceptance of the non-linear crystal. In this experimental project, the instrument is not fully fibered. The non-linear upconversion is not currently performed at the focus of the telescope, but at the end of each interferometric arm, just before the recombination of the fields. As a consequence we did not use any fibered delay line, but instead the CHARA Array delay lines. Thanks to a numerical model, we have found that the transmission coefficient of the CHARA Array, including its delay lines and the injection of light into the ALOHA single-mode fiber in H band, is around 5% for a seeing close to $1.1''$.

From these experimental results, we have developed a second numerical model to estimate the sensitivity of the ALOHA/CHARA instrument in its future interferometric configuration. In this framework, we found that for a seeing of $0.8''$, we should be able to detect fringes for a magnitude up

to +3.7 in H band, with a spectral resolution $R = 2600$. The simulation does not take the atmospheric turbulence into account, which may reduce the limiting magnitude.

The next step of this proof of principle study is to implement ALOHA at the CHARA Array in the interferometric configuration at 1.55 μm, and to get fringes during an on-sky observation. A trade-off between the coherence time of the atmospheric turbulence and the frame duration will be experimentally investigated. In the longer term, ALOHA will show its true potential for longer wavelengths. For example, PPLN crystals can be designed to convert optical fields from the K and L bands towards the near infrared, with a high spectral resolution and, in particular in the L band where low loss and long length single-mode fiber does not exist, an efficient spatial filtering after the SFG stage. Finally, in a very long term framework, the ALOHA concept extended to the M and N bands could be a promising prospect. By performing the upconversion process as close as possible to the telescope focus, we can envision a kilometric interferometer using optical fibers for coherent transport of light (Reynaud *et al.*, 1992; Delage and Reynaud, 2001). Moreover, the very high spectral resolution, inherent to the conversion process, allows us to consider the implementation of long fibered delay lines.

Acknowledgments

This work is supported by the Centre National d'Études Spatiales (CNES), the Institut National des Sciences de l'Univers (INSU), Leukos-systems and Thales Alenia Space. Operational funding for the CHARA Array is provided by the Georgia State University College of Arts and Sciences and by the National Science Foundation through Grant AST-1211129. We would like to acknowledge Alain Dexet for his advice and the realization of the mechanical parts.

References

Boyd, R. W. [2008] *Nonlinear Optics*, 3rd edn. (Academic Press, Amsterdam, Boston).

Brummelaar, T. A. T., McAlister, H. A., Ridgway, S. T., *et al.* [2005] *ApJ* **628**, 453, doi: 10.1086/430729.

Brustlein, S., Del Rio, L., Tonello, A. *et al.* [2008] *Phys. Rev. Lett.* **100**, 153903.

Ceus, D., Delage, L., Grossard, L. *et al.* [2013] *MNRAS*, doi:10.1093/mnras/sts654.

Ceus, D., Tonello, A., Grossard, L. *et al.* [2011] *Opt. Express* **19**, 8616, doi: 10.1364/OE.19.008616.

cleardarksky.com [2016] *Mount Wilson Observatory Clear Sky Chart History*, http://www.cleardarksky.com/clmt/c/MtWilsonOBCAct.html.

Coudé du Foresto, V. & Ridgway, S. T. [1992] "Fluor — A stellar interferometer using single-mode fibers", *European Southern Observatory Conf. and Workshop Proc.*, 731, http://adsabs.harvard.edu/abs/1992ESOC...39..731C.

Defrère, D., Hinz, P. M., Skemer, A. J. *et al.* [2015] *ApJ* **799**, 42.

Delage, L. & Reynaud, F. *et al.* [2001] *Opt. Express*, **9**, 267.

Gomes, J.-T., Delage, L., Baudoin, R., *et al.* [2014a] *Phys. Rev. Lett.* **112**, 143904, doi: 10.1103/PhysRevLett.112.143904.

Gomes, J. T., Grossard, L., Baudoin, R., *et al.* [2014b] *J. Astron. Instrum.* **3**, 1450008.

Lagarde, S., Robbe-Dubois, S., Petrov, R. G., *et al.* [2012] "MATISSE: Concept, specifications, and performances", (International Society for Optics and Photonics), 84452J, doi: 10.1117/12.926285.

Le Bouquin, J.-B., Berger, J.-P., Lazareff, B., *et al.* [2011] *A & A* **535**, A67, doi: 10.1051/0004-6361/201117586.

Leinert, C., van Boekel, R., Waters, L. B. F. M., *et al.* [2004] *A & A* **423**, 537, doi: 10.1051/0004-6361:20047178.

Pelc, J. S., Ma, L., Phillips, C. R., *et al.* [2011] *Opt. Express* **19**, 21445, doi: 10.1364/OE.19.021445.

Petrov, R. G., Malbet, F., Weigelt, G. *et al.* [2007] *A & A* **464**, 1, doi: 10.1051/0004-6361:20066496.

Reynaud, F., Alleman, J. J. & Connes, P. [1992] *Appl. Opt.* **31**, 3736, doi: 10.1364/AO.31.003736.

Scott, N. J., Millan-Gabet, R., Lhomé, E., *et al.* [2013] *J. Astron. Instrum.* **2**, 1340005, doi: 10.1142/S2251171713400059.

weather.gc.ca [2016] *Seeing Forecast for Astronomical Purposes*, http://weather.gc.ca/astro/seeing_e.html.